Nonlinear performances of dual-pump amplifiers in silicon waveguides*

Meng Fan(孟 凡)†, Yu Chong-Xiu(余重秀),
Deng Yun-Yi(邓云逸), and Yuan Jin-Hui(苑金辉)

State Key Laboratory of Information Photonics and Optical Communications (Beijing University of Post and Telecommunications), Beijing 100876, *China*

(Received 29 June 2011; revised manuscript received 26 October 2011)

The performances of a dual-pump parametric and Raman amplification process and the wavelength conversion in silicon waveguides are investigated. By setting the Raman contribution fraction f to be 0.043 in our analytical model, the amplification gain of the probe signal can be obtained to be over 10 dB. The pump transfer noise (PTN), the quantum noise (QN), and the total noise figure (TNF) are discussed, and the TNF has a constant value of about 4 dB in the gain bandwidth. An idler signal generated during the parametric amplification (PA) process can be used to realize the wavelength conversion in wavelength division multiplexing (WDM) systems. In addition, the pump signal parameters, the generated free carrier lifetime and effective mode area (EMA) of the waveguide are analysed for the optimization of signal gain and noise characteristics.

Keywords: silicon waveguide, parametric amplification, stimulated Raman scattering, noise figure, wavelength conversion

PACS: 42.25.Bs, 42.65.Dr, 42.65.Wi, 42.65.Yj **DOI:** 10.1088/1674-1056/21/4/044202

1. Introduction

It is well known that the fibers have been widely used in the areas of signal amplification[1−3] and wavelength conversion[4−7] for years, but the requirement for device minimization makes them awkward in optical information processing. During a long time period, the integrated optics have become more and more mature in the communication field.[8−11] As one of the semiconductor materials, silicon is used as the propagation medium and the substrate. Microelectronic techniques make it popular not only in electronic circuits, but also in optical chips and devices. In the state of the art, silicon can be used to make lasers,[9] modulators, microrings,[12] optical switches, and wavelength converters.[12]

When the intensity of incident waves is strong enough, nonlinear effects like four-wave mixing (FWM) and stimulated Raman scattering (SRS) occur and can be used to realize the signal amplification and the wavelength conversion.[13] Both the continuous waves (CW) and ultrashort pulse waves have been employed as pump signals to transfer the energy to the probe and idler signals. Compared with CW signals which require the lifetime of generated free carriers to be below 20 ps, the pulsed signals avoid measuring like ion implantation and applying a bias voltage to obtain the same gain level.[14,15] Amplifiers based on silicon can achieve more than 10-dB net gain in a length of several centimeters.[14] Dual-pump parametric amplifiers can achieve nearly 300-nm bandwidth[16] while the SRS induced Raman response peak wavelength in silicon has a frequency shift of 15.6 THz (124.8 nm at the wavelength around 1550 nm) from that of each incident signal. This means the peak wavelength is contained in the signal gain and wavelength conversion bandwidths, making them reduce greatly. Although Raman contribution fraction f in silicon is much smaller than that in silica fibers, SRS could still induce much more changes on the parametric amplification (PA) gain spectrum. The corresponding noise figures (NFs) of pump transfer noise (PTN) and quantum noise (QN), the total noise figure (TNF), and the wavelength conversion are also analysed. To optimize the properties of the waveguides, some parameters are discussed in detail.

*Project supported by the State Key Development Program for Basic Research of China (Grant No. 2010CB327605), the Discipline Co-construction Project of Beijing Municipal Commission of Education, China (Grant No. YB20081001301), and the Fundamental Research Funds for Central Universities, China (Grant Nos. 2011RC008 and 2009RC0314).

†Corresponding author. E-mail: mengfan3426@bupt.edu.cn

© 2012 Chinese Physical Society and IOP Publishing Ltd

2. Basic principle of analytical model

When two pumps with pulse signals and one probe signal are incident into a silicon waveguide, both PA and SRS occur. A set of amplitude coupled equations describing this amplification process can be given as follows:[1]

$$\frac{\mathrm{d}A_h}{\mathrm{d}z} = -\frac{(\alpha+\alpha_h^{\mathrm{F}})}{2}A_h + \mathrm{i}\Bigg[\left(\gamma+\mathrm{i}\frac{\beta}{2}\right)|A_h|^2 A_h + \varphi_1(z)A_h + 2\gamma\Bigg\{1-f+\frac{f}{2}(H(\omega_s-\omega_l) + H(\omega_i-\omega_l))\Bigg\}A_sA_iA_l^*\exp(\mathrm{i}\Delta\beta z)\Bigg], \tag{1a}$$

$$\frac{\mathrm{d}A_l}{\mathrm{d}z} = -\frac{(\alpha+\alpha_l^{\mathrm{F}})}{2}A_l + \mathrm{i}\Bigg[\left(\gamma+\mathrm{i}\frac{\beta}{2}\right)|A_l|^2 A_l + \varphi_2(z)A_l + 2\gamma\Bigg\{1-f+\frac{f}{2}(H(\omega_s-\omega_h) + H(\omega_i-\omega_h))\Bigg\}A_sA_iA_h^*\exp(\mathrm{i}\Delta\beta z)\Bigg], \tag{1b}$$

$$\frac{\mathrm{d}A_s}{\mathrm{d}z} = -\frac{(\alpha+\alpha_s^{\mathrm{F}})}{2}A_s + \mathrm{i}\Bigg[\left(\gamma+\mathrm{i}\frac{\beta}{2}\right)|A_s|^2 A_s + \varphi_s(z)A_s + 2\gamma\Bigg\{1-f+\frac{f}{2}(H(\omega_h-\omega_i) + H(\omega_l-\omega_i))\Bigg\}A_hA_lA_i^*\exp(-\mathrm{i}\Delta\beta z)\Bigg], \tag{1c}$$

$$\frac{\mathrm{d}A_i}{\mathrm{d}z} = -\frac{(\alpha+\alpha_i^{\mathrm{F}})}{2}A_i + \mathrm{i}\Bigg[\left(\gamma+\mathrm{i}\frac{\beta}{2}\right)|A_i|^2 A_i + \varphi_i(z)A_i + 2\gamma\Bigg\{1-f+\frac{f}{2}(H(\omega_h-\omega_s) + H(\omega_l-\omega_s))\Bigg\}A_hA_lA_s^*\exp(-\mathrm{i}\Delta\beta z)\Bigg], \tag{1d}$$

where $|A_k|$ $(k=h,l,s,i)$ are the wave amplitudes and ω_k $(k=h,l,s,i)$ are the angular frequencies,

$$\varphi_1 = (2-f)\gamma(|A_l|^2+|A_s|^2+|A_i|^2) + f\gamma(H(\omega_h-\omega_l)|A_l|^2 + H(\omega_h-\omega_s)|A_s|^2 + H(\omega_h-\omega_i)|A_i|^2), \tag{2a}$$

$$\varphi_2 = (2-f)\gamma(|A_h|^2+|A_s|^2+|A_i|^2) + f\gamma(H(\omega_l-\omega_h)|A_h|^2 + H(\omega_l-\omega_s)|A_s|^2 + H(\omega_l-\omega_i)|A_i|^2), \tag{2b}$$

$$\varphi_s = (2-f)\gamma(|A_h|^2+|A_l|^2+|A_i|^2) + f\gamma(H(\omega_s-\omega_h)|A_h|^2 + H(\omega_s-\omega_l)|A_l|^2 + H(\omega_s-\omega_i)|A_i|^2), \tag{2c}$$

$$\varphi_i = (2-f)\gamma(|A_h|^2+|A_l|^2+|A_s|^2) + f\gamma(H(\omega_i-\omega_h)|A_h|^2 + H(\omega_i-\omega_l)|A_l|^2 + H(\omega_i-\omega_s)|A_s|^2), \tag{2d}$$

where two-photo absorption (TPA) coefficient $\beta = 0.75\times10^{-11}$ m/W, free carrier absorption (FCA) coefficients $\alpha_k^{\mathrm{F}} = 1.45\times10^{-17}\,(\lambda_k/1550)^2 N$ $(k=h,l,s,i)$, and equations (2a)–(2b) contain cross phase modulation (XPM) and SRS. When $f=0.043$, the signal gain of parametric and Raman amplification is achieved.

At the output of the waveguide (propagation length is L), the probe signal gain $G(L)$ and idler wavelength conversion efficiency $C(L)$ are expressed as

$$G(L) = 10\lg(|A_s(L)|^2/|A_s(0)|^2)\ (\mathrm{dB}), \tag{3a}$$

$$C(L) = 10\lg(|A_i(L)|^2/|A_s(0)|^2)\ (\mathrm{dB}). \tag{3b}$$

The practical noise is mainly composed of two parts: PTN and QN, which stem from the pump signal intensity noise to probe signal gain and photon number fluctuation in optical gain, respectively. The TNF can be calculated by[14]

$$NF = 10\lg(NF_{\mathrm{PTN}} + NF_{\mathrm{QN}})\ (\mathrm{dB}). \tag{4}$$

3. Gain and noise characteristics

When PA without Raman process (case 1) is considered, the wavelength of the probe signal ranging from 1457 nm to 1663 nm is amplified greatly and the gain and the ripple are obtained to be more than 10.2 dB and smaller than 1 dB respectively as shown in Fig. 1., which is consistent with the result in Ref. [16]. In the PA with Raman process (case 2), two sharp peaks and one sharp valley appear on either side of the gain spectrum, which reduce the effective gain bandwidth by half compared with that in case 1. This phenomenon has already been demonstrated and depicted in Ref. [13]. The four obvious peaks are due to Raman scattering of the pump signals. As Raman frequency shift for silicon is 15.6 THz (124.8 nm), for the first pump (with a wavelength of 1512 nm), the Stokes wave is about 15.6 THz higher (1636.8 nm, close to 1641 nm), while the anti-Stokes wave is 15.6 THz lower (near 1402 nm). For the second pump (1591 nm), the

Stokes wave is 1734 nm and the anti-Stokes wave is 1470 nm. For sharp valleys, PA and SRS induce almost the same signal amplitudes but opposite phases, which offsets the probe signal power greatly after a short distance. Amplification spectrum is approximatively symmetric: gain characteristics in 1561 nm–1790 nm are almost the same as those in 1351 nm–1560 nm.

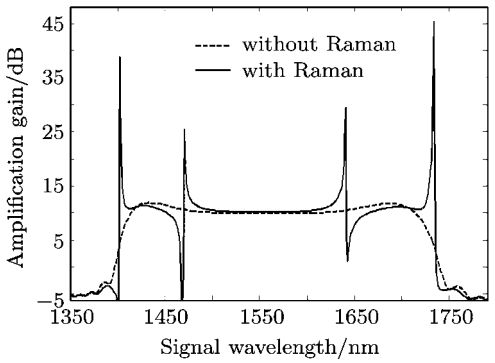


Fig. 1. Gain spectra without and with Raman effect.

Gain spectra, each as a function of probe wavelength and propagation distance, are shown in Figs. 2(a) and 2(b), where the formation of the signal gains can be seen clearly. In Fig. 2(b), the probe signal gain corresponding to some wavelength increases or decreases as it propagates in the waveguide. At the output end, the growth and the reduction accumulate up to a great extent, which result in the sharp gain peaks and valleys. Thus, this property can be used for the basis of lasing and filtering.

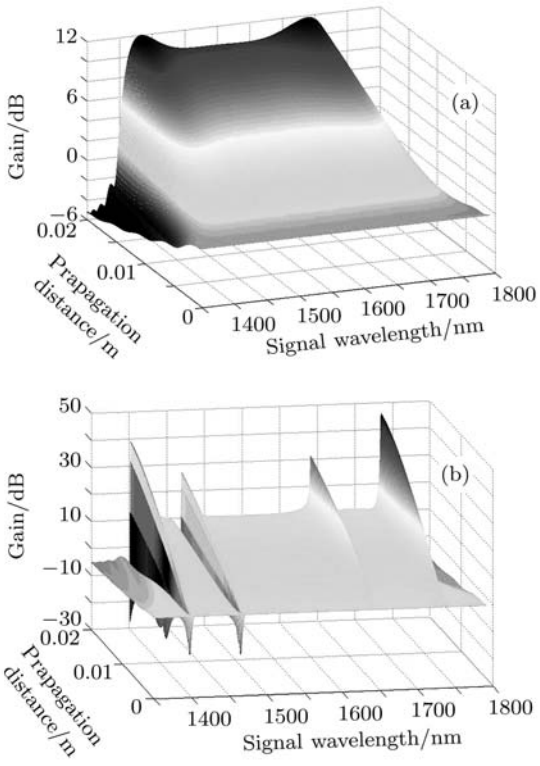


Fig. 2. Three-dimensional views of gain spectra each as a function of probe wavelength and propagation distance, PA without (a) and with (b) Raman effect.

Figures 3(a), 3(b), and 3(c) show PTN, QN, and TNF generated during the amplification process. As PTN is determined by the slope of net gain, its change is proportional to the gain spectrum. In the two cases, PTN is at a very low level under 0 dB, and shows vibrations on the edges of the spectrum. Since the phase mismatch on the edges of the gain bandwidth is large and unstable, a little change in pump power would

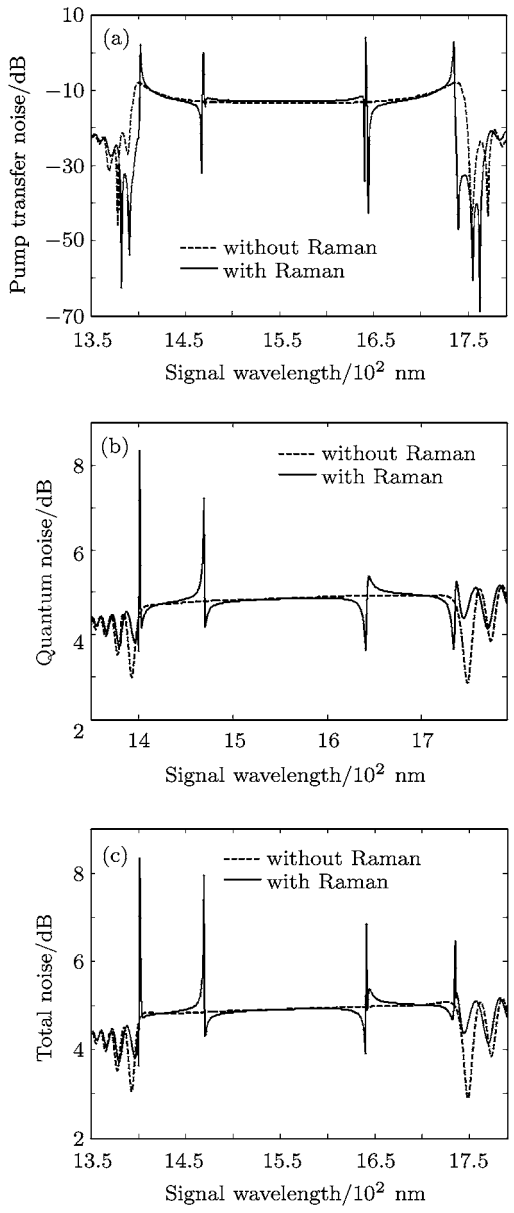


Fig. 3. Noise spectra of (a) PTN, (b) QN, and (c) TNF.

greatly affect the amplification gain. In Fig. 3(b), QN has an inverse correlation to the corresponding gain plot, which can counteract PTN sharp value to some degree. The QN stems from the gain coefficient $g(z)$ minus loss coefficient $l(z)$ integrating over each infinitely small length, and its average is more than 4.5 dB with ripple less than 0.2 dB, much larger than PTN. It may be noticed that the noise peak value induced by the anti-Stokes wave of the first pump is much higher than the other three, but in the gain plot it is not highest. This can be explained by the deep gain trench in its adjacent shorter range (seen from Fig. 2(b)), and the calculated integrals of $g(z)$ and $l(z)$ would cause a big QN peak at the wavelength near 1401 nm. Figure 3(c) shows that the TNF is determined mainly by QN, a flat TNF with a bandwidth in a range of 1491 nm–1631 nm and a ripple less than 0.1 dB is obtained. This TNF is a little higher than that of the single pumped scheme in Ref. [14], which can be understood easily.

4. Influence of pump signals and waveguide geometry

A light signal can generate free carriers through TPA in silicon,[17−21] and the generated carriers (electrons and holes) can in turn deplete it by FCA. At the same time, they can also influence the refractive index of the waveguide, which leads to free carrier dispersion (FCD). Unlike in silica fibers, all these special mechanisms in silicon make the amplification process much more complicated. So pump signals can affect the gain characteristics and NF at the same time. Figure 4(a) illustrates a pump signal and its generated free carriers, and the pump signal with a pulse width of 8.6 ps generates free carriers with a lifetime of 1 ns. When the pump signal is over in its pulse period, the free carriers need to take more time to annihilate, which remains affecting the probe and idler signals in the amplifying process.

Figure 4(b) shows the probe signal gain and noise (TNF) each as a function of the ratio of free carrier lifetime to pulse width at a probe wavelength of 1550 nm, while the carrier lifetime is fixed at 1 ns and pulse width varies from 1 fs to 100 fs. As the ratio increases, the gain increases rapidly and the noise decreases to a deep low level. When the ratio is larger than 200, both the gain and the noise are almost stable at 12.1 dB and 4.6 dB. However, when the pulse width is comparable to the carrier lifetime, the performance of the amplifier deteriorates greatly. These trends are similar to those of single-pump scheme[14] and dual-pump scheme[16] without Raman effect. Therefore, pump signals with ultrashort pulses are recommended.

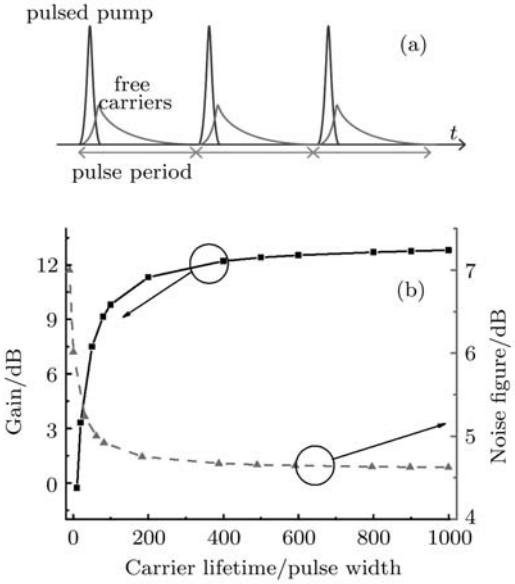


Fig. 4. (a) A general view of pulse waveform and generated free carrier lifetime each as a function of time, (b) gain and noise (TNF) each as a function of the ratio of free carrier lifetime to pulse width.

For better observation, the probe signal gain varying with both pulse width and bit rate of the pump signals is shown in Fig. 5. Bit rate from 1 GHz to 40 GHz and pulse width from 1 ps to 20 ps are chosen. When their values are small enough, the gain of more than 12 dB can be achieved. If net gain needs to be realized, it is necessary to choose the bit rate to be larger than 20 GHz and the pulse width below 7 ps, or pulse width larger than 16 ps and bit rate less than 8 GHz. So pump signals with lower bit rate and narrower pulse width are preferred to obtain a higher gain.[16]

Apart from the pump parameters, the geometry of the waveguide also has some influence on the gain characteristics of the probe signal.[22,23] Figures 6(a) and 6(b) show that the pump power and the probe gain vary with propagation distance, and the variation trends are opposite. As more pump power is depleted, more energy is transferred to the probe signal, which can be understood by physical insights. With the same pump parameters, four geometry distributions of effective mode area (EMA) are simulated. A

conclusion can be reached that the straight waveguide has the best performance in amplification process, the following waveguides are the hyperbolic geometry waveguide and the tilt waveguide has the lowest amplification gain.

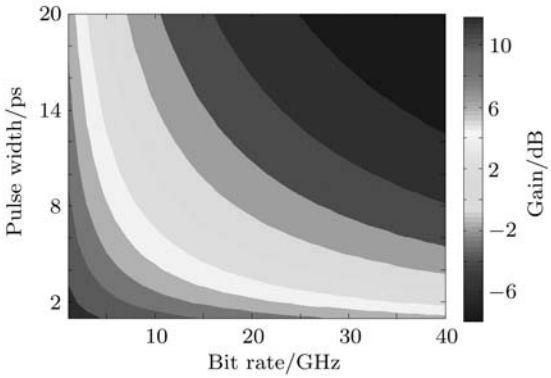


Fig. 5. Gain plot as a function of pulse width and bit rate of pump signals.

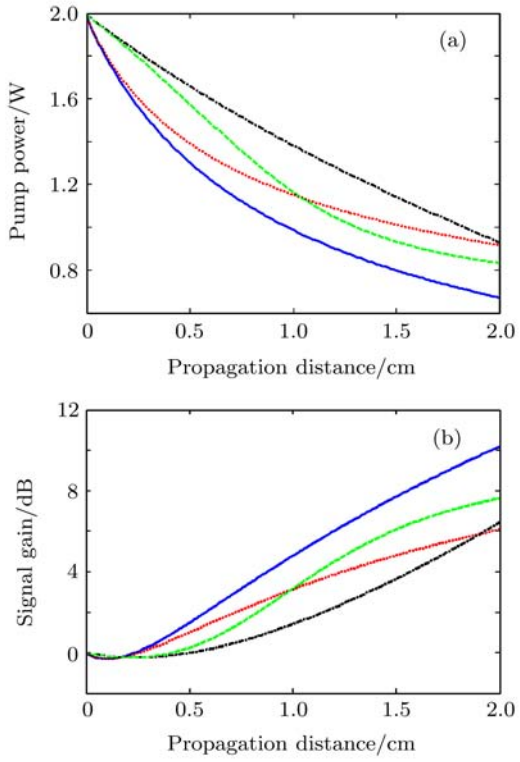


Fig. 6. (colour online) Pump powers (a) and probe gains (b) in different geometry distributions of effective mode area (EMA). solid-line (blue): straight waveguide with 0.38-μm^2 EMA; dot-line (red): tilt waveguide with 0.38-μm^2 EMA at the input end and 1-μm^2 at the output end; dash-dot line (black): tilt waveguide with 1 μm^2 EMA at the input end and 0.38 μm^2 at the output end; dash-line (green): hyperbolic waveguide with an area of 0.38 μm^2 in the middle and 1 μm^2 at the two ends.

5. Wavelength conversion

Apart from the probe signal amplification, the wavelength conversion of the idler signal in silicon waveguide can also be used in practice. Figure 7 shows the wavelength conversion efficiency as a function of probe signal wavelength in two cases, and this figure is much the same as that in Ref. [13]. Without Raman effect in case 1, the wavelength from 1419 nm to 1646 nm can be efficiently converted into the idler signal of 1465.5 nm–1708.8 nm with an efficiency of more than 10.1 dB and a ripple of smaller than 1 dB. Similar to the gain spectrum, SRS introduces four peaks and two valleys in the conversion bandwidth in case 2, which can also be explained by Stokes and anti-Stokes signal contributions. In case 2, the conversion bandwidth from 1482 nm to 1617 nm with an efficiency of more than 10.1 dB can be achieved, and the corresponding conversion bandwidth is 136.4 nm. The property is beneficial to the WDM system, since the silicon waveguides can be used as wavelength converters.

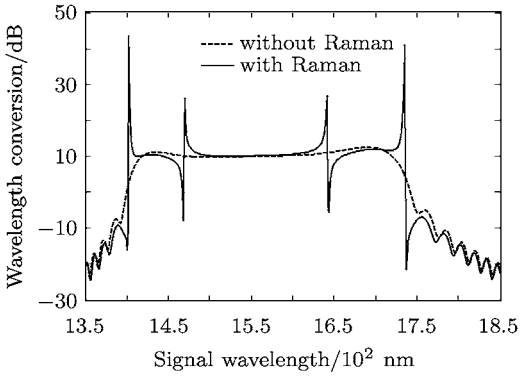


Fig. 7. Wavelength conversion efficiencies versus probe signal wavelength in two cases without and with Raman effect.

Figures 8(a) and 8(b) show the wavelength conversion efficiencies each as a function of probe signal wavelength (1351 nm–1790 nm) and propagation distance (2 cm) in two cases, respectively. Probe signals from 1351 nm to 1400 nm and 1741 nm to 1790 nm have a serious vibration along the propagation direction, which leads the corresponding conversion efficiency to be unstable. Considering the Raman effect in case 2, two idler signals corresponding to the probe signals of 1400 nm and 1402 nm respectively decreases and increases from the input end of waveguide and ends up with efficiencies of –16.09 dB and 43.59 dB. With a peak efficiency of 43.59 dB, a laser based on

wavelength conversion of PA with Raman effect can be designed.

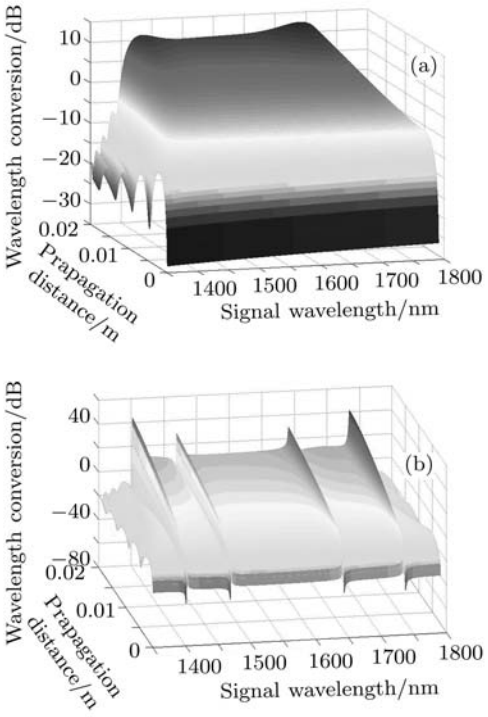


Fig. 8. Three-dimensional views of wavelength conversion efficiency as a function of probe wavelength and propagation distance. PA without (a) and with (b) Raman effect.

6. Summary

In this paper, a dual-pump signal parametric and Raman amplification in silicon waveguide is demonstrated. When two pump signals are employed, very broad signal gain and wavelength conversion bandwidth can be achieved. Raman scattering cannot be ignored since it introduces an obvious influence of Stokes and anti-Stokes gain peaks on both bandwidths. By setting the Raman contribution fraction $f = 0.043$ in coupled amplitude equations, the amplification gain, the noise characteristics, and the wavelength conversion efficiency are investigated. SRS introduces some vital influences of sharp peaks and valleys on both sides of gain bandwidth, so the corresponding PTN, QN, TNF, and wavelength conversion also show the similar properties. The values of signal gain, TNF, and conversion efficiency in the effective bandwidth are nearly independent of SRS, but their bandwidths are limited by SRS. Pulse width and bit rate of the pump signals, free carrier lifetime, and EMA distribution of the waveguide also have important influences on gain and noise characteristics, for they determine the nonlinear losses caused by TPA and FCA. With pump signals of lower bit rate (5 GHz) and narrower pulse width (3 ps), a probe signal gain of 12.1 dB and a noise of 4.6 dB can be achieved. These research results reveal the practical characteristics of dual-pump silicon waveguides.

References

[1] Boggio J M C, Moro S, Myslivets E, Windmiller J R, Alic N and Radic S 2009 *Proceedings of OFC*, March 22–26, 2009, Los Angeles, USA, p. 1

[2] Johan N and Bozena J 1993 *Opt. Lett.* **18** 2099

[3] Laurent P, Arnaud M, Eric L, Thibaut S and Hervé M 2003 *J. Opt. Soc. Am.* B **20** 1532

[4] Yuan J H, Sang X Z, Yu C X, Xin X J, Zhou G Y, Li S G and Hou L T 2010 *J. Optoelectron. Adv. Mater.-Rapid Commun.* **4** 23

[5] Yuan J H, Sang X Z, Yu C X, Li S G, Zhou G Y and Hou L T 2010 *IEEE J. Quantum Electron.* **46** 728

[6] Wang Y B, Xiong C L, Hou J, Lu Q S, Peng Y and Chen Z L 2011 *Acta Phys. Sin.* **60** 014201 (in Chinese)

[7] David A C, Christiano J S and Taylor J R 2002 *J. Opt. Soc. Am.* B **19** 1901

[8] Graham T R 2004 *Nature* **427** 595

[9] Liu A S, Rong H S, Richard J, Oded C, Dani H and Mario P 2006 *J. Lightwave Technol.* **24** 1440

[10] Koos C, Jacome L, Poulton C, Leuthold J and Freude W 2007 *Opt. Express* **15** 5976

[11] Liu A S, Liao L, Doron R, Hat N, Berkehan C, Yoel C, Nahum I and Mario P 2007 *Opt. Express* **15** 660

[12] Li W J, Sang X Z, Yu C X and Xin X J 2011 *J. Opt.* **13** 1

[13] Lin Q, Oskar J P and Govind P A 2007 *Opt. Express* **15** 16604

[14] Sang X Z and Boyraz O 2008 *Opt. Express* **16** 4786

[15] Liu Z X, Feng M, Guo Q H, Qiao L and Lu K C 2011 *Acta Phys. Sin.* **60** 014214 (in Chinese)

[16] Zhang Y, Sang X Z, Yang S Y, Rao L, Li W J, Yuan J H, Xin X J and Yu C X 2010 *Opt. Commun.* **283** 3043

[17] Fukuda H, Yamada K, Shoji T, Takahashi M, Tsuchizawa T, Watanabe T, Takahashi J and Itabashi S 2005 *Opt. Express* **13** 4629

[18] Ivan D R, Malin P, Chethiya D and Govind P A 2009 *Opt. Lett.* **34** 536

[19] Ivan D R and Indika U 2010 *Opt. Lett.* **35** 2343

[20] Lin Q, Zhang J D, Philippe M F and Govind P A 2006 *Opt. Express* **14** 4786

[21] Brian A D and Govind P A 2010 *J. Opt. Soc. Am.* B **27** 956

[22] Ivan D R, Chethiya D, Malin P and Govind P A 2009 *Opt. Express* **17** 5807

[23] Ivan D R, Chethiya D, Malin P and Govind P A 2010 *Selected Topics in Quantum Electronics* **16** 226